15th Australasian Wind Engineering Society Workshop
Sydney, Australia
23-24 February 2012

A Numerical Study of the Updrafts over a Building, with Comparison to Wind-Tunnel Results

A. Mohamed[1], C. White[1], and S. Watkins, [1]

[1]School of Aerospace, Mechanical and Manufacturing Engineering
RMIT University, VIC 3001, Australia

Abstract

There is an opportunity to utilise the updrafts of airflow over buildings for energy harvesting applications; such applications can include enhancing the flight duration of Micro Aerial Vehicles (MAVs) by the exploitation of the vertical velocity components, or locating the high velocity regions for the siting of wind generators. In this paper results from a numerical study are compared to a similar wind-tunnel study for the turbulent wind flow conditions around a representative building in an urban environment. The simulation involved a simplified model of a chosen representative building in an urban environment and was initially modelled in two-dimensions, using the standard k-ε turbulence model, which then evolved into a three-dimensional study which utilised the Large Eddy Simulation approach with Smagorinsky-Lilly sub-grid scale modelling. Using meteorological data, the Atmospheric Boundary Layer (ABL) velocity and turbulence intensity profiles were modelled at the inlet boundary of the computational domain, to recreate the same test conditions used in the wind-tunnel. It was found that the difference between the numerical model and the wind-tunnel data was less than 20% when comparing the updraft flow field. From the computed results, energy harvesting in the updraft region of buildings seem promising.

Introduction

Harvesting energy from the surrounding environment offers the potential to significantly increase range and endurance of Unmanned Air Vehicles (UAVs). Currently, there are UAVs that can harvest solar energy through solar panels, but the possibility of using naturally occurring thermals or updrafts as an energy source to gain height remains relatively unexplored. An early encouraging study by Allen, (2005) concluded that the endurance of a representative UAV could be increased by up to 12 hours by using thermal lift. The study presented by Wharington and Palmer, (2009) exploited thermals for autonomous soaring to increase UAV endurance and investigated optimisation of energy management strategies to improve performance of UAVs with wingspans of 2-8 meters. Further work by Edwards, (2008) demonstrated flight results of autonomous thermal soaring algorithms. Relatively unexplored is the use of slope or orographic lift (defined as lift that is created by the vertical motion of air moving past undulating terrain). Optimal flight trajectories for minimum flight time and maximum energy gain while crossing a ridge were also explored (Langelaan, 2007). Cutler et al., (2010) presented an important study into the feasibility of energy harvesting using orographic lift during intelligence, surveillance, and reconnaissance, (ISR) missions. This study showed when an energy source (such as a slope) is within 400 m of the target, no propulsive power was required for the selected UAV to orbit a target for ISR (the platform could maintain height using vertical component of the flow up the slope). The complex flow patterns that occur in suburban environments are typical for MAV operations, and can be beneficial for allowing an MAV to gain height and soar further or even recharge on-board batteries through regeneration. Watkins et al., (2010) states that MAVs need to operate around large obstacles and will be flying in the wake of buildings for some parts of missions. Understanding the flow patterns around buildings in suburban environments with particular attention to the updraft of airflow upstream of the building's roof top is therefore essential for MAV operations and energy harvesting applications.

Numeric models of the turbulent Atmospheric Boundary Layer (ABL) have been implemented for studying and analysing building envelopes, natural ventilation, wind loading, dispersion of air pollutants and other flow predictions (Tutar and Oguz, 2002). However, few if any studies have focused primarily on updrafts over rooftops. Most numerical studies focused on the general flow around single building models such as (Baskaran and Stathopoulos, 1989; Stathopoulos and Zhou, 1993; Paterson and Apelt, 1990; Murakami, 1990 1992) where the standard k-ε viscous turbulence model was implemented. Murakami et al, (1987); Murakami et al, (1990, 1993); Mochida et al, (1993) ; He and Song, (1992) used the Large Eddy Simulation approach. From these studies, the LES model seems to accurately predict the flow behaviour compared to the other models. There is also a rising number of studies investigating other building configurations such as that conducted by Baskaran and Kashef, (1996), where wind effects were investigated in a passage between two buildings. Lien et al, (2004) used the k-ε model to understand flow over a 2D array of buildings while Yik et al, (2010) have conducted 2D analysis of parallel ridges of varying height. To develop an understanding of the energy potentially available near the tops of buildings for endurance extension through soaring, velocity magnitudes will the need to be mapped in the region where updrafts are expected. Characterization of this updraft field will provide an indication of the energy availability for harvesting and inform MAV configuration and design.

Methodology

The representative building selected for the study presented in this paper is Building 201, (43 meters high and 38 meters wide) of RMIT University's Bundoora Campus (Melbourne Australia). The buildings' unique position and environment matched the topography of a suburban terrain. The average wind speed in Melbourne is around 11 km/h (3m/s) (Australian Bureau of Meteorology 2011). In a separate paper by White et al., (2011) a $1/100^{th}$ scale model of Building 201 was used for wind-tunnel testing and the results were validated by measurement from the roof of the actual building. The data from the wind-tunnel study is used for validation of the CFD results. The numerical study was conducted in 2D as a steady state problem, which then evolved into a transient 3D study. The 2D study allowed careful inspection of grid performance and domain size, which provides a basis for the 3D study. The 2D study has been simulated using the standard k-ε model with enhanced wall treatment, while the 3D study used the Large Eddy Simulation approach using the

Smagorinsky-Lilly model for sub-grid scale. 2D analysis has some inherent limitations where the 3D effects are neglected assuming the cross section being analysed is infinitely wide. This will result in some inaccuracy of the results since the flow around the building is expected to be highly three-dimensional.

The computational domain is constructed using a structured mesh. Very fine mesh resolution is used surrounding the building's vicinity, while the mesh size is increased with distance from the building boundaries. A mesh independence test was conducted allowing the selection of a mesh resolution that is computationally inexpensive while staying entirely within the linear sublayer to avoid the buffer region. The chosen mesh structure is a cartesian structured mesh. The un-skewed mesh offers accuracy in the analysis. The range of aspect ratio was checked and kept below 300. This mesh configuration was used for the 2D and 3D cases (see figure 1).

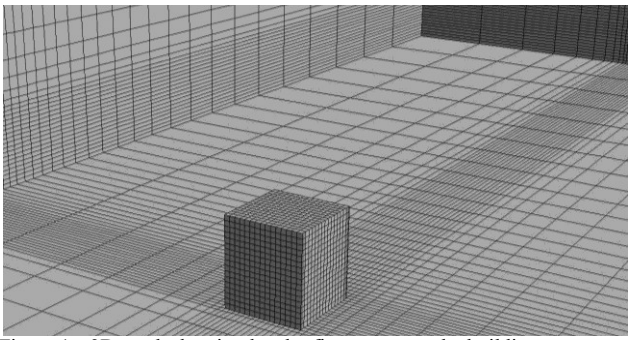

Figure 1. 3D mesh showing local refinement near the building.

Boundary conditions

The velocity profile at the inlet of the domain has been expressed as a power law and constructed using equation (3), the profile height changes according to the respective terrain case. From (Walshe, 1972), the values of a and z_g for a suburban terrain are 0.28 and 430 respectively.

$$\bar{u}_z = \bar{u}_g\left(\frac{z}{z_g}\right)^a \qquad (3)$$

The Reynolds number being simulated is 100,000 and therefore the corresponding fluid properties are summarised below.

$\rho = 1.22$ [kg/m3] (Density at building height [standard atmosphere])

$v = 1.574$ [m/s] (Average velocity at building height)

$l = 38$ [m] (Characteristic length of building)

$\eta = 7.3\text{x}10\text{-}4$ [kg/m s] (Air Viscosity)

Numerical Approach

The simulations presented in this report have been computed using FLUENT 6.3. This commercial solver, is a finite volume code with cell center collocated variable arrangement. As recommended by FLUENT's User Guide, the central-differencing scheme was employed for the spatial discretization in the high fidelity analysis presented. This scheme is ideal for improving the accuracy of the LES calculations. A Second order temporal discretization with non-iterative time advancement (NITA) was adopted. The iterative time-advancement scheme is computationally expensive unlike the NITA scheme which skips the requirement to compute many global iterations performed for each time-step, allowing for a single global iteration. The NITA method allows a significant benefit in computational time for transient simulations, compared to the iterative transient solution method. With the NITA scheme, the Fractional Step Method (FSM) is slightly less computationally expensive compared to the PISO algorithm as explained in the User Guide and was therefore selected. Generally, the default solution control values in FLUENT are enough to set a robust convergence of the internal pressure correction sub-iterations, arguably for most linear problems, but because the simulation presented is expected to show highly turbulent flow, it is sensible to reduce the under-relaxation factors. Under-relaxation factors were consequently set as; pressure: 0.7, momentum: 0.7. The simulations were computed using 24 nodes of a Linux-64 based VPAC cluster. The Fluent node selected system for interconnection is Infini-Band. The fluid properties are assumed to be constant for all simulations.

Results & Discussion

Two-dimensional Results

The default convergence criteria were deactivated in FLUENT and convergence was determined by monitoring the drag force on the building. Once the oscillation of the drag force reduced to a straight line, the simulation was considered convergent and the iterations were stopped . The flow features of the simulation show agreement with predicted behaviour and work previously published by researchers. Please note that all the presented results are normalised to the buildings reference height, H_b. Consequently the scales of the contours can be viewed as velocity ratios to the wind speed at H_b. The flow stagnates on the front face of the building at a height of 24.4m, therefore causing reversed flow at the base (figure 2a). The buildings sharp edge allows flow separation which reattaches 23.9m away from the buildings edge. There is also reversed flow over the roof top leading to recirculation. As predicted, the updraft region contains the highest magnitude of velocity. The y-axis velocity contour shows the y component of the flow's velocity near the rooftop. With the zero velocity clearly identified on the contour, it can be seen where there are updrafts and down-drafts. Regions with strong updrafts are visible in figure 2b. This is the region of interest for MAV flight.

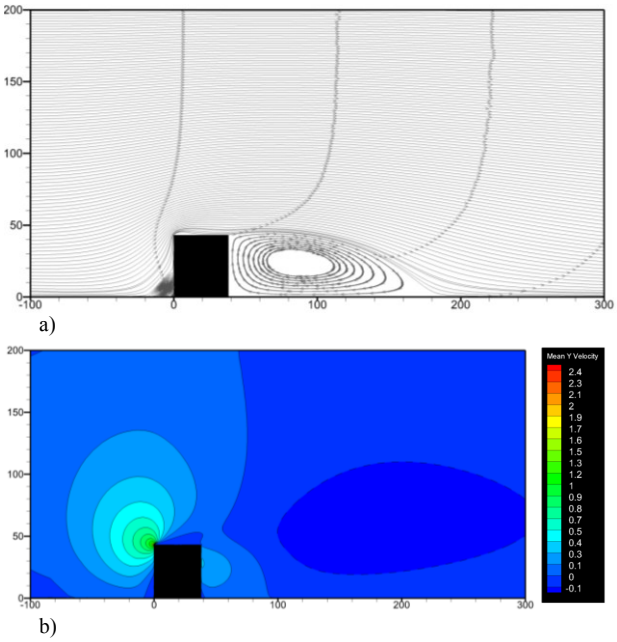

Figure 2.
a) 2D averaged streamline plots
b) 2D averaged y-velocity contours in ms^{-1}

Three-dimensional Results

The 3D results showed highly turbulent flow upstream, while downstream there is significant vortex shedding. A point in the wake behind the building was selected for monitoring the pressure fluctuation with time-step advancement, and

determining convergence of the model (figure 3). The plot was clipped off in the vertical axis where initially the solution was still converging. It is clear that the simulation starts to follow a re-occurring behaviour after a non dimensional time-step of ~40 signalling a developed flow pattern and therefore convergence. Consequently, statistics were turned on at a non dimensional time-step of 45, for averaging the results. The results presented have also been normalised to H_b.

The flow features of the 3D simulation also show agreement with the work previously published by researchers, as the basic flow features were replicated. As predicted, the updraft region contains the highest magnitude of vertical velocity at the roofs edge. Reattachment over the roof top occurs at 24.9m while behind the building occurs at 47.8m. Stagnation occurs at a height of 30.6m. Figure 6 shows the velocity contours, while the streamline plot is shown in figure 4. It's important to note that the contours are positioned on the lateral center of the building (i.e. at z = 0). In order to visualize the 3-Dimensionality of the updraft region and its core strength, an iso-surface was created showing 4 different core intensities (see figure 5).

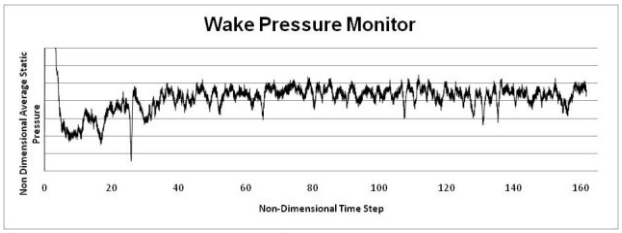

Figure 3. 3D Case pressure monitor.

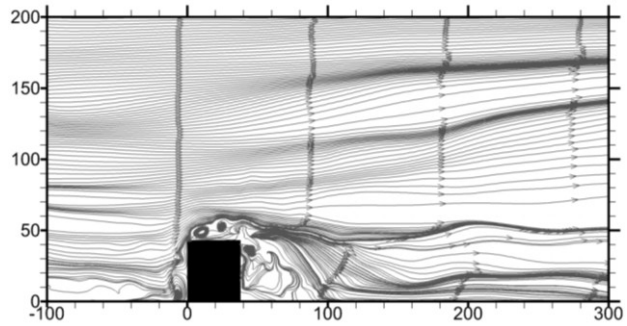

Figure 4. 3D Instantaneous streamline plots.

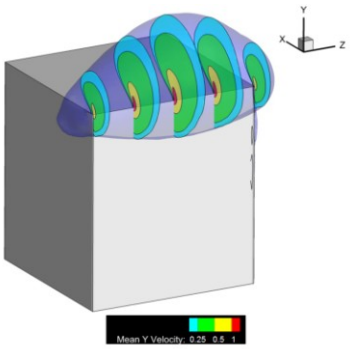

Figure 5. Iso-Surface showing 3 levels of mean vertical velocity.

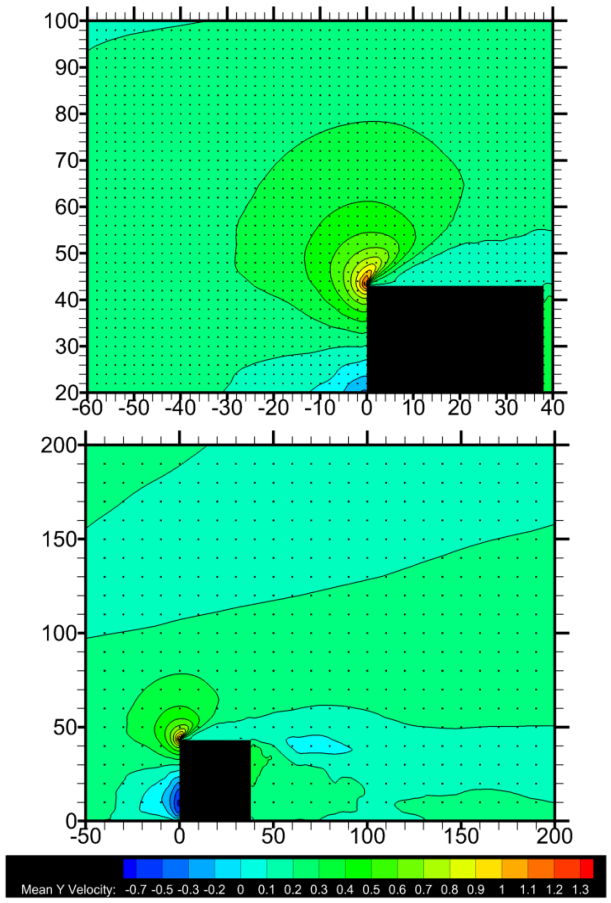

Figure 6. 3D mean vertical velocity contours.

Wind-tunnel Comparison

The same building geometry was tested in the wind tunnel at 1/100th scale with similar velocity and turbulence intensity profiles as presented by White et al., (2011). The wind-tunnel experiment used cobra probes to measure the velocity vectors in a spacial matrix in the vicinity of the building's rooftop. The same matrix was created in the domain of the numeric study for vector magnitude and direction comparison as illustrated in figure 7 . Both sets of results presented have been normalised to H_b.

It was observed that for the majority of the results, the difference was below 20%. This difference was expected because of a number of reasons. The velocity profile tested in the wind tunnel had a slightly varied shape compared with the theoretical profile used in the numerical analysis. The variation was due to the roughness elements installed in the wind-tunnel to replicate the ABL. The wake from those roughness elements also affected the stagnation location on the face of the building as observed from figure 7, where the vectors at a height of 34.5m show almost stagnant flow in the case of the experimental results. Even the simulated Reynolds Number tested in the wind-tunnel was different. The magnitude of the vectors is also different because the free stream velocity was about 3 times higher in the wind-tunnel experiment, which will also affect the flow angle upstream. table 1 summarises some of the flow features of the test cases and the wind-tunnel experiment.

Bldg 201 flow features	K-e	LES	Wind-tunnel
Roof Reattachment[m]	23.9	24.9	26.1
Ground Reattachment[m]	112.6	47.8	54.6
Stagnation Point[m]	24.4	30.6	≈35

Table 1. Result comparison summary

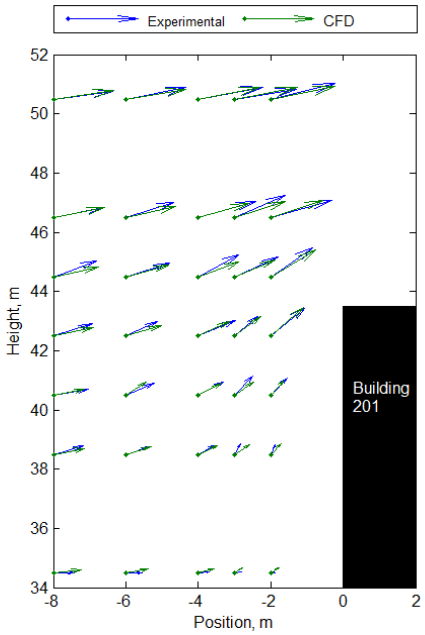

Figure 7. Velocity vector comparison.

Conclusion

The results obtained from the 2D analysis showed that in general, the CFD model has accurately represented the flow behaviours as previously published. The 2D analysis was essential in allowing sensitivity studies to be conducted for initiating the 3D analysis. The 3D analysis showed significant vortex shedding and highly turbulent flow entering the domain which was a phenomenon that wasn't captured by the 2D case. When comparing results it is evident that the 2D case over-predicted the updraft region while the 3D case provided results more representative of those obtained from wind-tunnel testing. The LES approach gave reliable results compared with the *k-ε* model and with increased computational power and a finer mesh resolution, this numerical approach will accurately recreate the ABL and predict velocities in the updraft region over buildings with greater accuracy. Although the results of the wind-tunnel and CFD where tested at different conditions the difference in results was nominally 20%. This discrepancy was due to the different Reynolds number tested in the wind-tunnel and also from the experimental error and over-predicted velocity profile in the wind-tunnel testing. Difficulties in numerical simulation of turbulent flow around buildings is another contributing factor.

References

Allen, M J (2005) Autonomous Soaring for Improved Endurance of a Small Uninhabited Air Vehicle, AIAA No. 2005-1025

Baskaran A, Stathopoulos T (1989) Computational evaluation of wind effects on buildings, Building Environment Vol 24 (4), pp 325-333.

Baskaran A, Kashef A (1996) Investigation of Air Flow Around Buildings Using Computational Fluid Dynamics Techniques, Engineering Structures

Cutler M J, McLain T W, Beard R W, Capozzi B (2010) Energy Harvesting and Mission Effectiveness for Small Unmanned Aircraft, AIAA

Edwards D J (2008) Implementation Details and Flight Test Results of an Autonomous Soaring Controller, AIAA Guidance Navigation, and Control Conference Vol 2008-7244

He J, Song C C S (1992) Computation of Turbulent Shear Flow Over Surface Mounted Obstacle, ASCE Journal of Engineering Mechanics

Langelaan J W (2007) Long Distance/Duration Trajectory Optimization for Small UAVs, AIAA Guidance, Navigation and Control Conference Vol 2007-6737

Lien F S, Yee E, Cheng Y (2004) Simulation of Mean Flow and Turbulence of a 2D Building Array Using High Resolution CFD and a Distributed Drag Flow Approach, Journal of Wind Engineering and Industrial Aerodynamics

Mochida A, Murakami S, Shoji M, Ishida Y (1993) Numerical Simulation of Flowfield Around Texas Tech Building by Large Eddy Simulation, Journal of Wind Engineering and Industrial Aerodynamics Vol 46-47, pp 455-460

Murakami S (1990) Computational Wind Engineering, Journal of Wind Engineering and Industrial Aerodynamics

Murakami S, Mochida A, Hayashi Y, Sakamoto S (1992) Numerical Study on Velocity-Pressure Field and Wind Forces for Bluff Bodies by k-ε, ASM, and LES, Journal of Wind Engineering and Industrial Aerodynamics

Murakami S, Mochida A, Hibi K (1987) Three-Dimensional Numerical Simulation of Airflow Around a Cubic Model by Means of Large Eddy Simulation, Journal of Wind Engineering and Industrial Aerodynamics Vol 25, pp 291-305.

Murakami S (1993) Comparison of Various Turbulence Models Applied to Bluff Body, Journal of Wind Engineering and Industrial Aerodynamics

Murakami S, Mochida A (1990) A 3-D Numerical Simulation of Air Flow Around a Cubic Model by Means of the k-ε Model, Journal of Wind Engineering and Industrial Aerodynamics

Paterson D A, Apelt C J (1990) Simulation of flow past a cube in a turbulent boundary layer, Journal of Wind Engineering and Industrial Aerodynamics

Stathopoulos T, Zhou Y S (1993) Numerical Simulation of Wind-Induced Pressures on Buildings of Various Geometries, Journal of Wind Engineering and Industrial Aerodynamics

Tutar M, Oguz G (2002) Large eddy simulation of wind flow around parallel buildings with varying configurations, Fluid Dynamics Research.

Walshe D E J (1972) Wind-Excited Oscillation of Structures, Her Majesty's Stationery Office

Watkins S, Thompson M, Loxton B, Abdulrahim M (2010) On Low Altitude Flight through The Atmospheric Boundary Layer, International Journal of Micro Aerial Vehicles

Wharington J, Palmer J (2009) UAV Performance Improvement through Autonomous Soaring, 3rd Australasian Unmanned Air Vehicles Conference.

White C, Lim E W, Watkins S, Mohamed A, Thompson M (2011) A Feasibility Study of Micro Air Vehicles Soaring Tall Buildings, Journal of Wind Engineering and Industrial Aerodynamics. (Submitted for Publication)

Yik L C, Salim S M, Chan A, Cheong C S (2010) CFD Study of Flow Over Parallel Ridges With Varying Height and Spacing, World Congress on Engineering